Geomorphology 320 (2018) 98–110

Contents lists available at ScienceDirect

Geomorphology

journal homepage: www.elsevier.com/locate/geomorph

Evaluation of DEM size and grid spacing for fluvial patch-scale roughness parameterisation

Jane Groom *, Stephane Bertin, Heide Friedrich

Department of Civil and Environmental Engineering, University of Auckland, Auckland, New Zealand

ARTICLE INFO

Article history:
Received 26 January 2018
Received in revised form 8 August 2018
Accepted 10 August 2018
Available online 12 August 2018

Keywords:
Grain-roughness
DEM
Parameterisation
Close-range photogrammetry

ABSTRACT

Surface roughness is a term used in fluvial research without a unanimous definition. Clarification of the term and improved parameterisation is needed in future research. Improvements to the collection of topographic data, using photogrammetry, have provided accurate digital elevation models (DEMs) of field and laboratory gravel-bed patches of varied sediment size and surface structure. In this study, a moving-window process is used for analysing spatial variability within DEMs. Using this information, and in unison, the effect of DEM size and grid spacing are considered on an extensive range of roughness parameters, in order to provide insights for obtaining grain-roughness statistics. It is shown that DEM size influences the calculated roughness statistics, and the observation of plateaus in statistics for DEM window sizes above $16 \times D_{50A}$ in both directions (where D_{50A} is the median grain size of the bed-surface material) suggests this as a minimum DEM size for grain-scale roughness analysis. Further, the DEM grid spacing should be 1 mm or below, in order to adequately capture grain roughness, as coarser resolutions failed to detect particle imbrication. Finally, variability in roughness parameters was evident due to natural spatial variation in gravel-bed microtopography, suggesting using a single roughness parameter is not appropriate to holistically describe the roughness of a gravel patch. As the importance of topographic information continues to grow in geomorphology, the results of this study will assist researchers in the collection and subsequent analysis of DEMs.

1. Introduction

Calls to re-evaluate the term for roughness and improve parameterisation in future research have been made (Lane, 2005; Rice et al., 2014; Martinez-Agirre et al., 2016), due to the term being used frequently, albeit with little definition (Morvan et al., 2008; Jia and Hu, 2015).

Surface roughness in fluvial environments such as gravel-bed rivers influences the dynamic interactions between flow, sediment transport and ecology (Aberle and Nikora, 2006; Hodge et al., 2009a; Baewert et al., 2014; Curran and Waters, 2014). Previous parameterisation of roughness included subjective estimations of coefficients or the use of roughness heights based on grain size and velocity profiles (Wilcock, 1996; Smart et al., 2004). However quantitative roughness parameters are now obtained, including bed-elevation moments such as standard deviation, skewness and kurtosis determined from transects or digital elevation models (DEMs) (Aberle and Nikora, 2006).

Research on gravel-bed rivers now gathers information collected from 'patch-scale' DEMs for roughness parameterisation, although studies differ in data collection (e.g., the size and resolution of measurements) and analysis (e.g., detrending method and roughness parameters used). Therefore, explicit definitions of a gravel patch and patch-scale DEMs are still lacking; yet, it is understood the size and resolution of measurements should allow for adequate representation of the surface character (Hodge et al., 2009a). Roughness parameters are used as inputs for both hydraulic and morphodynamic models, including determining flow resistance (Aberle and Smart, 2003; Tuijnder and Ribberink, 2012). Measurements of bed topography (e.g., the standard deviation of bed elevations) are also helpful for obtaining estimates of sediment size on the bed surface (see Pearson et al., 2017 for a review). Therefore, accurate parameterisation of surface roughness is required to avoid error propagation in several applications of fluvial science and modelling (Smart et al., 2002; Lane, 2005; Morvan et al., 2008).

This analytical paper aims to provide insights into patch-scale gravel-bed DEM analysis for obtaining roughness information. A combination of laboratory and field data are used, allowing for generalizable results, with the application of a moving-window analytical process and the consideration of an extensive range of roughness parameters. Firstly, this study considers roughness spatial variability to comprehend topographic signatures of water-worked gravel beds and their analytical requirements. Previous research considered the small-scale spatial variability in grain size (Crowder and Diplas, 1997), with applications

* Corresponding author.
E-mail addresses: jgro800@aucklanduni.ac.nz (J. Groom), h.friedrich@auckland.ac.nz (H. Friedrich).

https://doi.org/10.1016/j.geomorph.2018.08.017
0169-555X/

to evaluate the effect of sampling area on the accuracy of image-based grain size measurements (Graham et al., 2010), and to explain spatial differences in grain entrainment (Piedra et al., 2012). Recent work presented new results on the spatial variability and scaling of surface structure (i.e., topography) in gravel-bed rivers, allowing for the isolation of roughness scales from DEMs (Bertin et al., 2017). This paper continues on this emerging avenue of research, with a wider selection of roughness parameters assessed. Secondly, using information on roughness spatial variability, this paper assesses the combined effect of DEM size and grid spacing on output roughness parameters. This analysis is relevant to all researchers, who want to ensure the adequate selection of DEM size and grid spacing for their study. The current scope of literature in relation to each of these objectives is discussed in more detail in the background section following.

2. Background

An overview of the procedure for analytical processes considered throughout this study is provided in Fig. 1. This visually presents the different analytical steps investigated, including the effect of DEM size (i.e., the spatial extent of the DEM or measured patch, Step 1) and grid spacing (equivalent to DEM resolution, Step 3). Complete details of the processes will be outlined in the methodology section.

2.1. DEM size

Roughness values are dependent on a suitable DEM size, as this determines the scale over which the roughness is calculated (Florinsky and Kuryakova, 2000; Smith, 2014). Research on grain roughness suggests that the size of the gravel patch measured needs to be large enough to capture a range of sediment sizes, including several large grains (Hodge et al., 2009a). However, a more quantitative guideline for the size of a DEM is required (Step 1, Fig. 1), as patch-scale research has used DEM sizes ranging from 0.1 m^2 to 1 m^2 (Hodge et al., 2009a; Mao et al., 2011; Ockelford and Haynes, 2013; Rice et al., 2014). Recent literature deemed patch sizes, which equate to 21 × D_{50} in both directions, suitable for analysis of grain roughness changes for flows below entrainment threshold (Ockelford and Haynes, 2013). Unfortunately, reasons behind this decision were not presented and it is not clear if D_{50} refers to the bulk mixture or bed surface sediment, which is problematic when grain size varies between surface and subsurface, such as for armoured beds.

Previously, a moving-window approach (Step 4, Fig. 1) was used to determine the grain-size variability of a river reach (Crowder and Diplas, 1997), and to evaluate DEM error spatial distribution for various survey strategies and interpolation methods (Heritage et al., 2009; Milan et al., 2011). Further, studies in different applications, including large scale floodplain analysis, have altered the DEM size (using a moving-window technique, with a window radius ranging from 1 m to 1000 m), which allowed for the identification of threshold sizes for DEMs to produce topographic metrics (Florinsky and Kuryakova, 2000; Scown et al., 2015). These papers highlight the importance of establishing the scale of interest in order to select a suitable DEM size.

Recent use of moving windows of different sizes on gravel patches distinguished roughness signatures of grains and bedforms (Bertin et al., 2017). Contrasting with grain roughness, measures of bedform roughness did not always reach stable values with window-size increases, suggesting that patch-scale DEMs may be limited in use to the analysis of grain roughness (Bertin et al., 2017; Powell et al., 2016). Just like Graham et al. (2010) using grain-size spatial variability for examining the effect of sampling area on the accuracy of grain size measurements, previous research suggests that knowledge on roughness spatial variability can provide guidance towards an appropriate DEM size for analysis of surface roughness, which will be evaluated in this study.

2.2. DEM grid spacing

Future research using high resolution data needs to consider the level of detail required for the application (Smith, 2014). For example, the grid spacing (i.e., DEM resolution) used when converting a point cloud to a DEM (Step 3, Fig. 1) also determines the scale over which roughness is calculated, with previous studies stating patch-scale investigations require higher resolution and precision (Smith et al., 2012; Smith, 2014). Studies at various scales from soil properties, gravel surfaces and catchment landscapes, have found that changes in measurement resolution influence the obtained roughness values or topographic parameters and affect DEM accuracy (Zhang and Montgomery, 1994; Smith, 2014; Trevisani and Cavalli, 2016; Grieve et al., 2016; Bertin and Friedrich, 2014; Lane et al., 2000; Gao, 1998; Erskine et al., 2007; Milenković et al., 2015; Barber et al., 2016). Thus the scale of the process investigated should influence grid spacing choice.

Studies on gravel beds have used grid spacing including 0.1 mm, 1 mm and 5 mm, regardless of sediment size on the patch (Buffin-Bélanger et al., 2006; Ockelford and Haynes, 2013; Hodge et al., 2009a; Bertin and Friedrich, 2014; Curran and Waters, 2014). Due to this range, it is important to investigate the effect of a resolution below, and above, the 1 mm resolution commonly used for gravel patches, in order to provide an indication to the optimal grid spacing for use in grain roughness analysis.

3. Methodology

3.1. Gravel-bed patches and digital elevation models (DEMs)

DEMs representing the microtopography of five gravel-bed patches from different geomorphic settings (i.e. collected from both the field and a laboratory flume) were used for the study (Fig. 2).

Three DEMs collected in August 2014 from the Whakatiwai River, a small gravel-bed stream located in New Zealand North Island, and presented in Bertin and Friedrich (2016), form the field surfaces. Patches from three exposed and vegetation-free gravel bars (labelled "Field 1" to "Field 3", with numbers increasing upstream) were selected for measurements, covering a range of sediment size and surface structure (Table 1). Each patch was selected at the bar head close to the water edge, for both consistency in the measurements, and ensuring the surfaces are regularly water-worked under similar hydraulic conditions.

Two armoured gravel beds called "Lab 1" and "Lab 2" formed in a non-recirculating tilting flume with glass side-walls (19 m long, 0.45 m wide and 0.5 m deep), with a flume slope set at 0.5%, are also examined. The experimental beds were obtained from water-working two distinct sediment mixtures. A constant flow rate of 84 L/s (mean flow velocity = 0.82 m/s, shear velocity = 0.077 m/s and uniform water depth = 0.225 m) was applied until the rate of sediment transport dropped to <1% of the initial transport rate. Both sediment mixtures were prepared from distinct but slightly bimodal alluvial sediments (15% sand and 85% gravel, and 9% sand and 91% gravel, respectively), with size ranging from 0.7 to 35 mm (Table 1). The tests were performed under condition of sediment starvation (i.e., no sediment feeding).

To allow the accurate measurement of the bed-surface topography and grain structure with digital photogrammetry for the five patches, a pair of Nikon D5100 cameras (16.4 Mpixel, 23.6 × 15.6 mm^2 sensor size) with Nikkor 20 mm lenses, was installed in stereo (horizontal baseline distance between cameras between 0.25 and 0.3 m) vertically (i.e., both cameras looking down, minimising occluded points which cannot be seen in one or the two images) above the gravel beds.

The photogrammetric technique employed herein to obtain DEMs from stereo photographs (i.e., two overlapping images as shown in Step 1, Fig. 1) consists of (i) in-situ calibration, using the method of

Step 1: Data acquisition

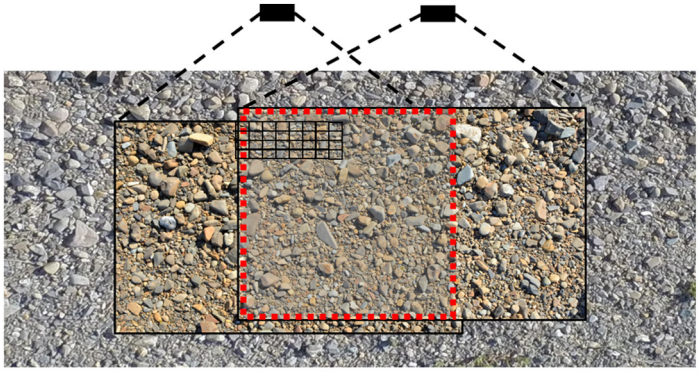

Photogrammetry; where the common field of view (CFoV) (overlap in two images) determines the patch size (red dashed line) for analysis.

Pixel size (small black squares) determined by sensor size, focal length and camera distance.

Step 2: Data processing

Stereo matching

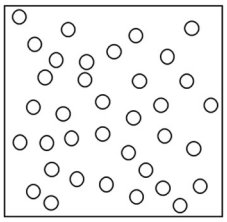

Point cloud with a resolution determined by pixel size and size determined by CFoV.

Step 3: Generation of DEM

Interpolation onto regular grid (e.g. determining grid spacing)

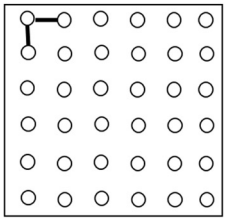

DEM maximum size (e.g. patch size) determined by CFoV and grid spacing (thick black lines) is ≥ pixel size which can be user defined.

Step 4: Detrending

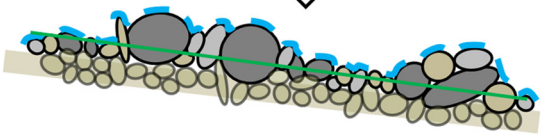

DEMs are detrended using flat-surface detrending to remove the effect of bed slope or experimental setup (green line), which otherwise could obscure the grain roughness of interest (blue dashed line).

Step 5: Moving-window analysis

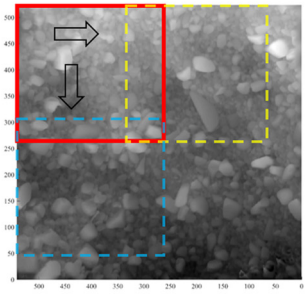

Roughness parameters (presented in Table II) are calculated for each window whilst windows are moved across the entire DEM. For each parameter, statistical analysis consists in measuring the median, standard deviation and coefficient of variation (CV).

Black arrows indicate moving window in both directions. New windows defined with coloured dashed lines.

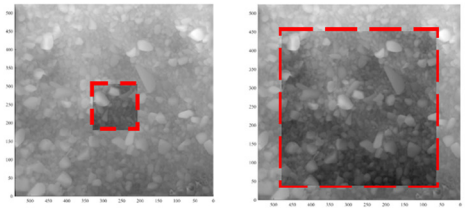

The procedure is repeated for different window sizes.

Example depicts 4 x D_{50A} (left) or 16 x D_{50A} (right) in both directions.

Fig. 1. Overview diagram of the generation of topographic data using digital photogrammetry and analytical processes discussed further, including interpolation using varying grid spacing and a moving window technique.

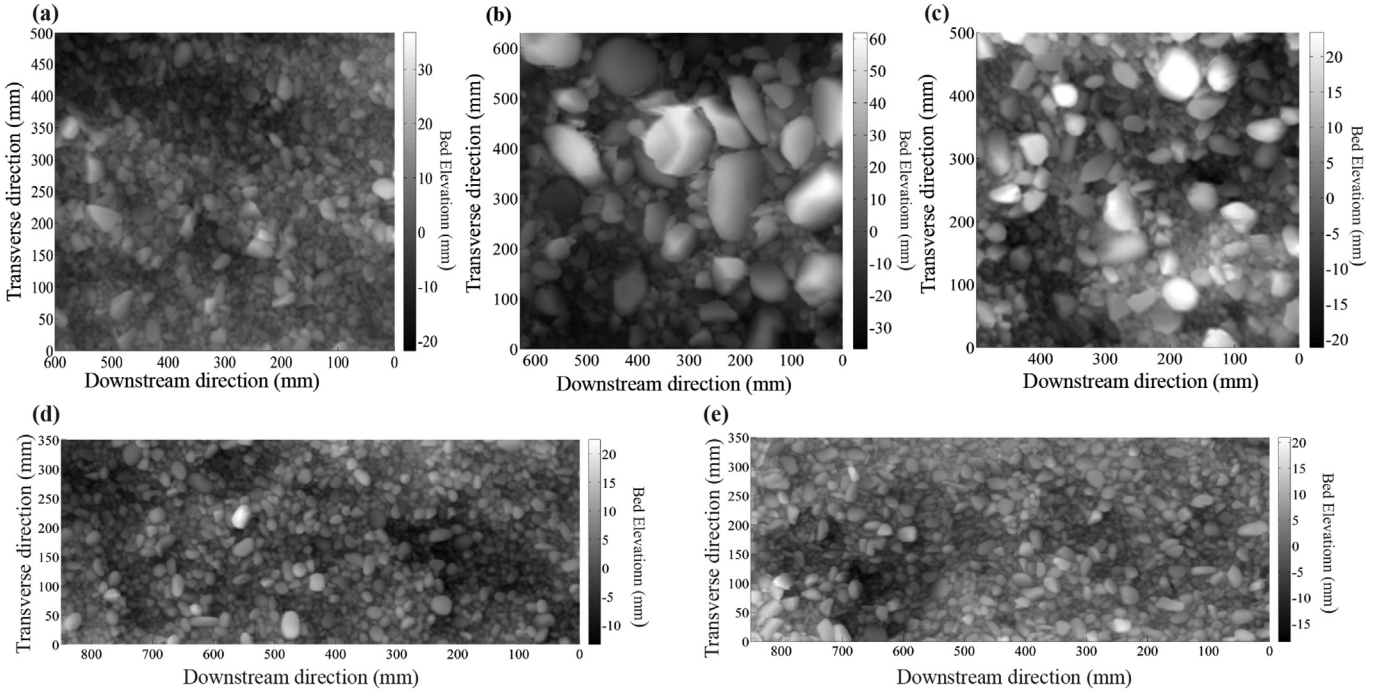

Fig. 2. Digital elevation models (DEMs) displaying the gravel-bed surfaces around the mean bed level, after flat-surface detrending, by removing the combined effect of bed slope and setup misalignment: (a) Field 1; (b) Field 2; (c) Field 3; (d) Lab 1 and (e) Lab 2. The surface forming flow direction is right to left.

Zhang (2000), included in Bouguet's (2010) open-access calibration toolbox for Matlab®, which requires several stereo photographs of a planar chequerboard to be recorded to determine both intrinsic (i.e., camera) and extrinsic (i.e., setup) calibration parameters; (ii) using the calibration data to accurately rectify (mean rectification error < 0.5 pixel and maximum error < 1 pixel throughout the imaging area) stereo photographs of the gravel beds to epipolar geometry, whereby corresponding pixels between overlapping images are ideally on a same scanline (i.e., corresponding pixels have the same y-coordinate); (iii) scanline-based pixel-to-pixel stereo matching using Gimel'farb's (2002) symmetric dynamic programming stereo (SDPS) algorithm, providing both point cloud data and ortho-images (Step 2, Fig. 1). Using the SDPS, occluded points are interpolated based on the assumption of a continuous surface, leaving no voids. The careful design of the measurement setup (e.g., adjusting the baseline and the camera height to the relief of the surface) helps to minimise occlusions (Lane et al., 2000; Bertin et al., 2015); yet determining the proportion of occluded points is not possible. To fulfil analytical requirements of regularly-spaced data (e.g., to measure bed-elevation structure functions) and to avoid bias introduced by non-uniform data when calculating the standard deviation of bed elevation σ_z (Hodge et al., 2009a), point clouds were interpolated (using the triangle interpolation method in Matlab) onto regular grids (i.e., raster DEMs as shown in Step 3, Fig. 1) with spacing 1 mm (the reference grid spacing against which other grids are compared, see Section 3). Each DEM underwent rigorous quality assurance testing (readers can refer to Bertin et al. (2015) and Bertin and Friedrich (2016) where detailed evaluations of the laboratory and the field DEMs are presented, respectively), to ensure surface metrics derived from the DEMs had minimum effect due to DEM errors. Outliers, which accounted for <1% of the DEM points, were identified using the mean elevation difference parameter by comparing each DEM point with its direct neighbours (Hodge et al., 2009b), and replaced using bi-cubic spline interpolation. All DEMs were finally normalised to have a mean bed level equal to zero, and rotated to be aligned with the surface-forming flow direction. Whilst flow direction identification is straightforward for laboratory surfaces, the flow direction for field

Table 1
Summary of the GSD information (both surface and subsurface where applicable) and DEM characteristics, for the five gravel-bed patches. The subscript 'A' indicates surface sediment from the armour layer, rather than the bulk sediment. The best DEM horizontal resolution is the average pixel size on the gravel beds, which is also the average point spacing in point clouds. The theoretical vertical error is estimated using classical photogrammetric equations and depends on camera and lens specifications (i.e., sensor size, number of pixels and focal length), as well as setup characteristics (i.e., baseline and camera distance). True DEM accuracy (here the mean unsigned error) was estimated using a 3D-printed gravel-bed model to be 0.43 mm and 0.67 mm in the laboratory and the field, respectively (cf. Bertin and Friedrich, 2016).

	Field 1	Field 2	Field 3	Lab 1	Lab 2
D_{50} (mm)	N.A.	N.A.	N.A.	8.4	9.2
$\sigma_G = \sqrt{D_{84}/D_{16}}$	N.A.	N.A.	N.A.	3.0	2.6
D_{50A} (mm)	18.7	47.2	19.4	18.9	18.5
D_{90A} (mm)	27.3	104.7	47.7	27.1	28.1
$\sigma_{GA} = \sqrt{D_{84A}/D_{16A}}$	1.4	2.2	2.3	1.4	1.4
Patch size (mm) (downstream × transverse)	600 × 500	630 × 630	500 × 500	850 × 350	850 × 350
Normalised patch size by D_{50A} (downstream × transverse)	32 × 26	13 × 13	25 × 25	45 × 18	45 × 18
Best DEM horizontal resolution (mm)	0.20	0.22	0.19	0.17	0.16
Theoretical vertical error (mm)	0.55	0.59	0.47	0.36	0.36
Approximate camera distance (mm)	825	860	765	675	670

data was determined by eye from observations of channel shape and grain imbrication (Laronne and Carson, 1976; Millane et al., 2006; Bertin and Friedrich, 2016). Finally, using a least-squares fit, flat-surface detrending was undertaken to remove the influence of both the bed slope and experimental setup misalignments from the DEMs (e.g., Aberle and Nikora, 2006; Bertin and Friedrich, 2016).

As shown in Table 1, camera height could not be set constant throughout both the field and the laboratory applications. The DEM characteristics therefore varied slightly between applications, although DEM resolution and vertical error remained small compared to sediment size (cf. Table 1), a precondition for grain roughness characterisation (Hodge et al., 2009b). One can note that the laboratory DEMs have larger coverage, yet smaller pixel size and theoretical vertical error. This is because the laboratory DEMs were obtained by merging three smaller overlapping DEMs, allowing shorter camera distance. We note that other measurement techniques such as laser scanning (Hodge et al., 2009a, 2009b; Aberle and Nikora, 2006) have been used by others to produce gravel-bed DEMs similar to the ones used in this study.

3.2. Grain-size distributions (GSDs)

To complement topographic information derived from DEMs and to allow comparison with sediment size, the bed-surface composition based on the sediment grains' intermediate axis was determined for each gravel patch using a single vertical photograph (number of detected grains >400) and the image-analysis tool Basegrain®. The latter allows for automatic grain separation in digital images of gravel beds and applies the Fehr's (1987) line-sampling method for results' analysis (Detert and Weitbrecht, 2012). Independent measurements were obtained by measuring surface sediment along lines with a digital calliper (with results presented in Stähly et al. (2017)), which allowed us to calibrate the results obtained with Basegrain.

In addition to surface composition determined with Basegrain, the experimental sediment mixtures used in the laboratory were sieved to determine the sediment grading curves (Table 1), particle shape and specific gravity. To distinguish GSDs of the bed surface from those of the bulk mixtures, percentiles derived from GSDs were indexed with "A" to represent characteristics of the armoured surface.

3.3. Grid spacing and the effect of DEM horizontal resolution

To quantify the effect of DEM resolution or grid spacing on the roughness information derived, point clouds of the five patches were transformed into DEMs of varying resolution by interpolating the raw elevation data (using triangle interpolation in Matlab) from point clouds on regular grids (Step 3, Fig. 1) with spacing: 0.35 mm, 0.5 mm, 1 mm (the reference grid spacing), 3 mm, 10 mm, D_{50A} and $2 \times D_{50A}$ (i.e., spacing equal to the surface median grain size and two times the surface median grain size, respectively). The decision on the grid spacings used herein was guided by grid spacings used in the literature (as presented in the background section), as well as to enable investigation of a threshold grid size decoupled from sediment size (here D_{50A}, as this is the property most commonly reported).

3.4. Surface metrics and the moving-window analysis

To quantify the character and surface variability of the five patches, six surface metrics (see Table 2) were calculated for each DEM within moving windows of different sizes. In reporting the experiments, the term DEM size is used to refer to two things, which is worthy of clarification: (i) DEM size refers to the size of the gravel patch measured, which is a 'constant' for each patch and is presented in Table 1; (ii) DEM size is then altered using moving windows, and we use our measurements of roughness spatial variability for different window sizes to identify a minimum DEM size for roughness analysis. The maximum window size testing is therefore less than the patch size.

Square windows were used (in comparison to circular windows as in Scown et al., 2015), since recorded DEMs are more often square (or rectangular) in shape. The effect of the measurement orientation (in the case of rectangular DEMs) was also examined. For this, the initially square windows were halved either horizontally or vertically to form rectangular windows with their long axis aligned either parallel or perpendicular to the flow direction. To facilitate observations from the graphs and to allow comparison between the five patches studied, window size in both directions was normalised by D_{50A} (i.e., calculations were made within windows with an area proportional to the area covered by the surface D_{50A} determined over the whole DEM). Surface metrics were obtained for each window of the designated size, whilst windows are moved across the whole surface of the DEM (Step 4, Fig. 1), with the number of windows fitting into the DEM ranging from >2000 (at small window sizes) to <50 (at larger window sizes). An overlap between moving windows of 95% of the window size was used, except for calculating structure functions, for which a 25% overlap was used due to the very large computational demand (still, a typical run time was 24 h per DEM). Sensitivity analysis of the effect of changing the overlap size to 25% showed no adverse effect interpreting the findings. However, a 95% overlap was preferred when possible due to refined visual presentations of the results across window sizes (i.e., smoother graphical lines).

The commonly used surface metrics calculated from bed-elevations used in this study are presented in Table 2. Bed-elevation distribution moments contained in probability distribution functions (PDFs) include

Table 2
Surface metrics calculated from gravel-bed elevations used in this study.

Parameter	Formula	Equation
Standard deviation (σ_z)	$\sigma_z^2 = \frac{1}{N'}\sum_{i=1}^{N'}(Z_i - \langle Z_i \rangle)^2$	(1)
Skewness (S_K)	$S_k = \frac{1}{N'\sigma_z^3}\sum_{i=1}^{N'}(Z_i - \langle Z_i \rangle)^3$	(2)
Kurtosis (K_u)	$K_u = \left[\frac{1}{N'\sigma_Z^4}\sum_{i=1}^{N'}(Z_i - \langle Z_i \rangle)^4\right] - 3$	(3)
Structure function (D_{G2})	$D_{G2}(\Delta x, \Delta y) = \frac{1}{(N-n)(M-m)}\sum_{i=0}^{N-n}\sum_{j=0}^{M-m}\{\lvert z(x_i + n\delta x, y_j + m\delta y) - z(x_i, y_j)\rvert\}^2$	(4)
Inclination index ($I0$)	$I0 = \frac{n_+ - n_-}{Ns}$	(5)

z represents the bed elevation at location (x,y) in a DEM, N′ is the total number of DEM points and ⟨ ⟩ represents the mean value. $\Delta x = n\delta x$ and $\Delta y = m\delta y$; δx and δy are the sampling intervals (i.e., DEM resolution) in the longitudinal and transverse directions respectively; $n = 1,2,3,\ldots N$ and $m = 1,2,3,\ldots M$. N and M are the number of DEM points in the same two directions. n_+ and n_- are the number of positive and negative slopes between successive DEM points, respectively, and Ns is the total number of slopes.

σ_z, S_K and K_u and are classic descriptors of bed roughness used in a number of studies at scales ranging from grain size to channel shape (e.g., Aberle and Nikora, 2006; Scown et al., 2015). Surface variability about the mean elevation within an area is indicated by σ_z (Eq. (1)) and represents a characteristic vertical roughness scale of the bed surface, which can be used as a grain-roughness parameter in flow resistance equations (Aberle and Smart, 2003; Noss and Lorke, 2016). Skewness (S_K, Eq. (2)) describes the degree of asymmetry of the PDF and can be used to assess the general shape of the bed surface. In this regard for water-worked gravel beds, a positive skewness is attributed to finer grains filling depressions and reducing the magnitudes of surface deviations below mean bed level (Aberle and Nikora, 2006). Kurtosis (K_u, Eq. (3)) provides a measure of the regularity or intermittency of the bed. A distribution characterised by heavy tails and a narrow peak has a large kurtosis, with more of the variance due to infrequent extreme deviations. More uniform and compact distributions, of frequent modestly sized deviations from the mean, are of lower kurtosis values (Coleman et al., 2011).

Horizontal roughness lengths in both the streamwise and the cross-stream direction (L_x and L_y, respectively) are scaling characteristics of a surface and are calculated from second-order structure functions (Eq. (4)). Structure functions, which are different from semivariograms by a factor two, measure changes in elevation correlations at different spatial lags and in different directions (Fig. 3). Small structure function values represent regions characterised by similar elevations (because of DEM points located on a same grain or bedform), while large values identify regions on a surface that are not correlated anymore. A gravel-bed elevation structure function has three regions: a scaling region with uniform slope at small lags, a saturation region at large lags, where the slope is zero, with a transition region in between, where the slope decreases (Nikora et al., 1998; Hodge et al., 2009a). As shown in Fig. 3, the scaling region of the 1D structure function fitted with a power law, provides information about the horizontal roughness lengths L_x and L_y, which are determined from the slope breakpoint, located at the intersection between the tangent to the scaling region slope and the saturation level asymptote, in both x and y directions (Nikora et al., 1998). Hence, L_x and L_y were calculated from 1D structure functions whereby $\Delta x = 0$ and $\Delta y = 0$, respectively. The maximum spatial lag to calculate D_{G2} (Eq. (4)) in both x and y directions was chosen as half the window size in the same two directions, and L_x and L_y were determined at the condition the saturation region was attained for all moving windows of the same size.

The inclination index (*I0*) in the flow direction is calculated using Eq. (5) (Smart et al., 2004). It analyses the signs of elevation changes between successive pairs of DEM points on transects aligned with the flow direction at a lag distance equal to the DEM resolution, where a positive slope refers to increasing bed elevations downstream. Slopes whose absolute value is below 0.01 were deemed not reliable (i.e., neither positive nor negative), and were therefore not counted in the numerator of Eq. (5) (Millane et al., 2006). A positive inclination index reflects the dominance of positive slopes and thus particle imbrication, generally maximum in the flow direction, minimum in the direction opposite to the flow, and approximately zero in a direction transverse to the flow (Laronne and Carson, 1976; Millane et al., 2006). Characterising grain imbrication is therefore relevant for determining flow direction from bed-surface analysis, but also provides insights on bed stability and the history of the flow that shaped the surface.

The surface variability for the six surface metrics was also quantified with the coefficient of variation (CV), calculated as the standard deviation of the property determined over all moving windows divided by the mean, and expressed as a percentage. To study the effect of measurement scale on surface variability, CV was calculated for different window sizes.

4. Results

Because the respective effects of DEM size and grid spacing on roughness parameters cannot be presented collectively, examination is undertaken step-by-step. Starting with the effect of DEM size, the spatial variability of roughness parameters using moving windows is examined. Only window size is altered during this first part of the

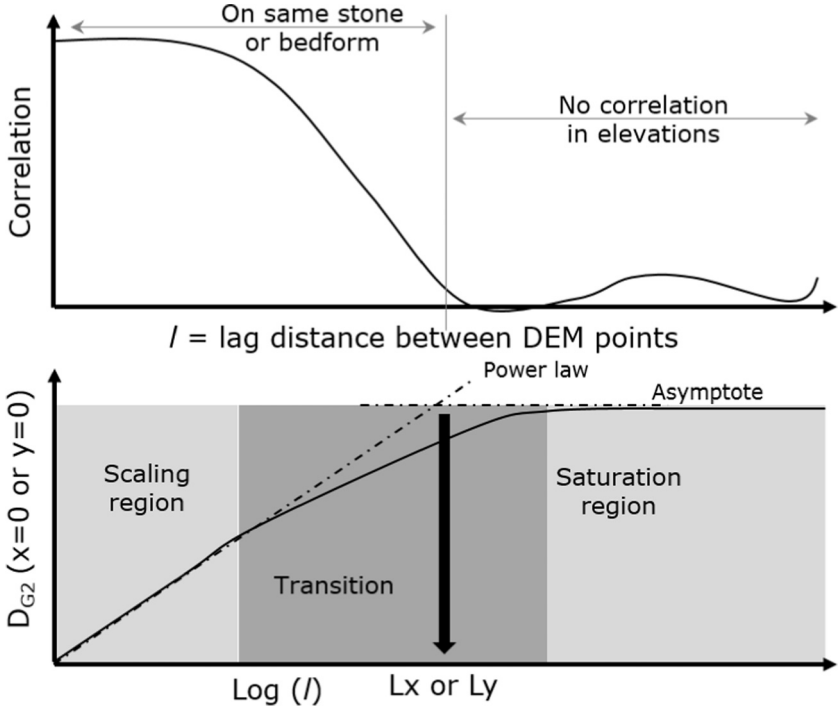

Fig. 3. Typical gravel-bed elevation correlation and structure function graph for different spatial lags, used to determine horizontal roughness lengths *Lx* and *Ly*. Adapted from Smart et al. (2002).

analysis, while generic grid spacing is maintained (i.e., grid spacing equal to the reference value of 1 mm).

4.1. Roughness spatial variability

Fig. 4 presents the coefficient of variation (CV) for all roughness parameters and gravel patches considered in this paper with changes in moving-window size. As is common practice, CV was used at the condition of positive property values only. Here, the surface metrics S_K and *I0* sometimes adopt negative values when calculated over small window sizes, whilst positive values (characteristic of a water-worked and imbricated gravel bed) are measured for all patches at larger window sizes. Therefore, calculation of CV for S_K and *I0* required adjustments in the range of window sizes, as shown. Despite this caveat, two observations can be obtained from Fig. 4. Firstly, there are differences in the spatial variability of certain roughness parameters. Particularly evident are the higher CV values at a given window size, in both skewness and inclination index, an indication that these two parameters vary widely spatially within a gravel patch. Across all DEMs, the parameters which provided the lowest CV values (reaching a minimum

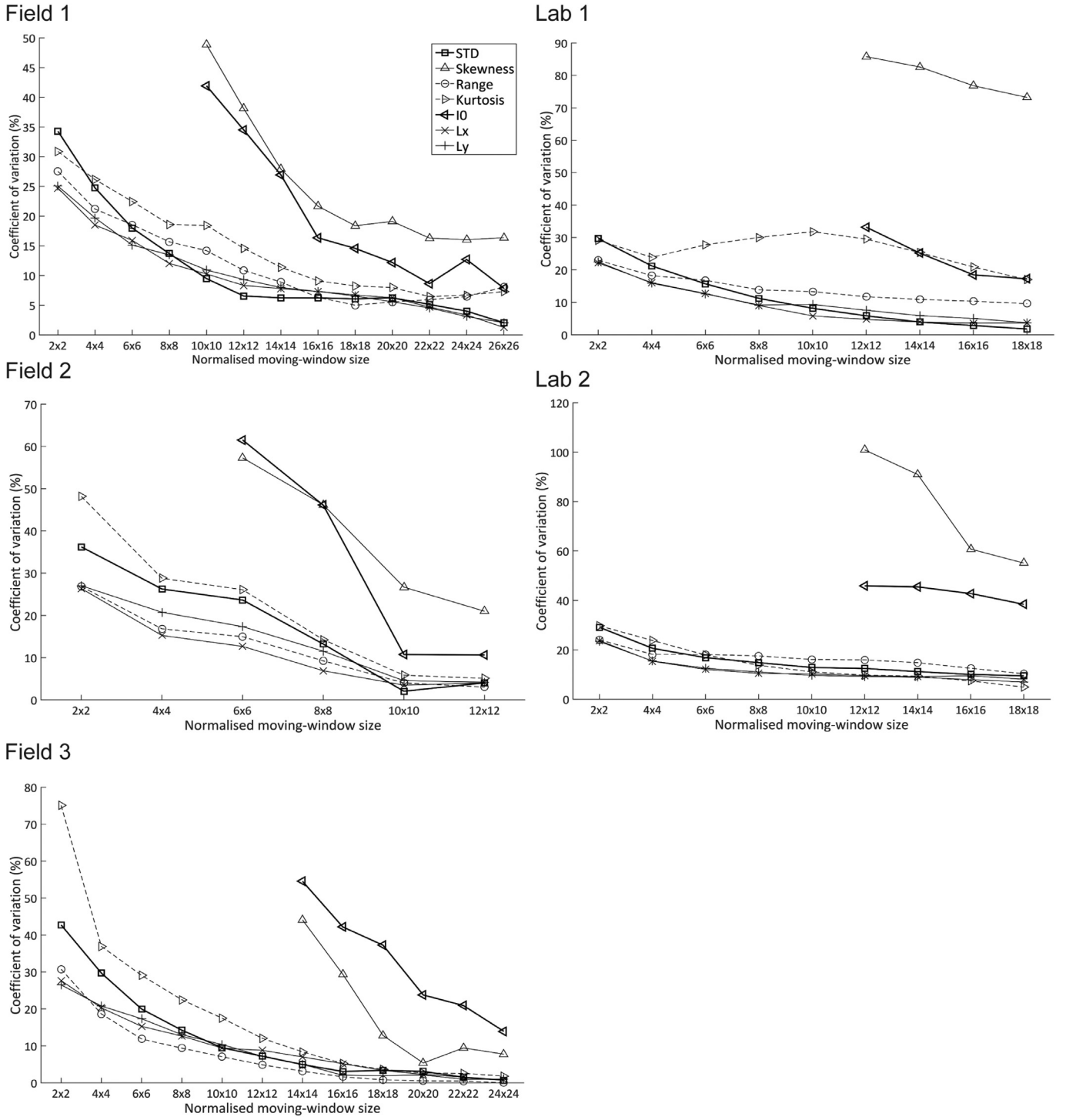

Fig. 4. Coefficient of variation (CV) for all roughness parameters, for all datasets (Field DEMs left column, Lab DEMs occupy the right column), calculated at different moving-window sizes normalised in both directions by D_{50A}.

of below 5%), were horizontal roughness lengths L_x and L_y, along with σ_z (Fig. 4). Secondly, spatial variability for the majority of roughness parameters declines with increases in moving-window size, until it plateaus out. Similar to the findings of Scown et al. (2016) at the scale of a floodplain, this observation suggests the existence of a threshold DEM size, evaluated hereinafter, above which the surface roughness of the patch is characterised by the parameters and decision on the location of the DEM within the patch is becoming less important.

For the rest of the analysis, not all roughness parameters are presented, but instead horizontal roughness lengths, σ_z, and *l0* are chosen to exemplify trends representative of all roughness parameters. The selection comprises roughness parameters commonly used for gravel

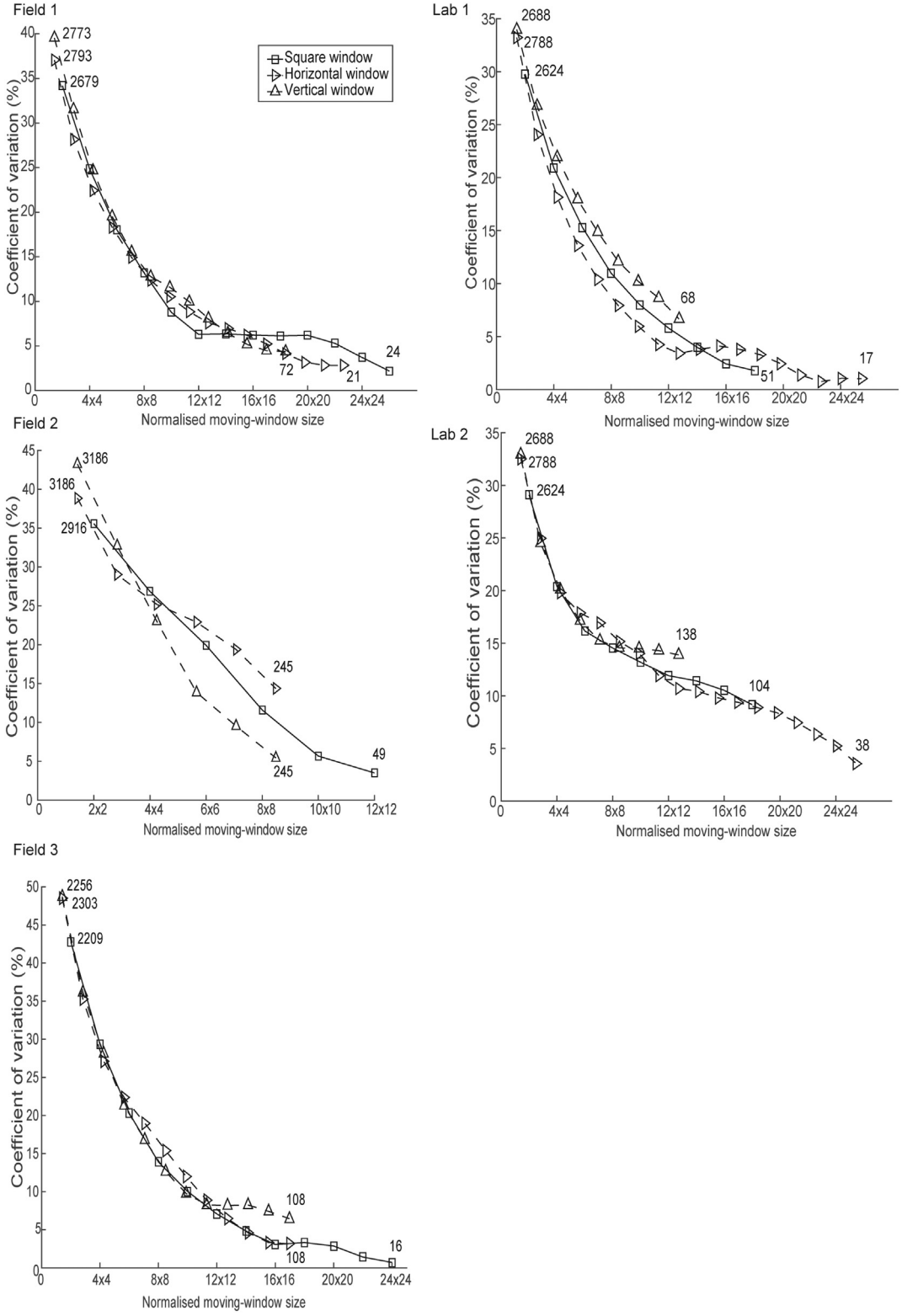

Fig. 5. Coefficient of variation (CV) in σ_z for all datasets (Field DEMs left column, Lab DEMs occupy the right column), calculated at different moving-window sizes normalised in both directions by D_{50A}. The number of windows generated for the maximum and minimum sizes are provided on the graphs.

beds and as shown in Fig. 4, encompasses parameters with a wide range of spatial variability, therefore maximising the representativeness of the findings.

4.2. Effects of DEM size and orientation on roughness parameterisation

Fig. 5 displays the coefficient of variation (CV) in σ_z for all five datasets. Previously, we observed a consistent decrease in spatial variability with window size increases for all roughness parameters studied (Fig. 4). Focusing on one parameter now enables examination of whether a threshold DEM size represented by a plateau in variability exists, as well as to examine the effect of patch orientation.

Fig. 5 confirms a clear effect of window (hence DEM) size on the roughness statistics, for all patches. The smaller the moving-window size, the larger the variance in results produced across the patch. Variance reduces and plateaus as the window size increases, between 12 and 18 × D_{50A} across the majority of the patches. However, there are patches showing a further decrease in variance following this observed plateau (Fig. 5a and c). Given bedforms were not filtered from DEMs for this analysis; this observation suggests two spatial scales of surface roughness present, namely grain and bedform roughness (Bertin et al., 2017).

Across all patches the size of the window (hence DEM size) has a greater control on roughness statistics than the orientation of the window. Similarities in statistics exist regardless of the orientation (shape) of the window, apart from Field 2 (Fig. 5b), where vertical windows result in lower CV, and Lab 1 (Fig. 5d), where CV is higher for vertical windows and lower for horizontal windows compared to the use of square windows. These differences suggest surface anisotropy in the flow direction for Lab 1, whilst Field 2 is characterised by higher variability in σ_z in the transverse direction.

Boxplots obtained using the moving-window analysis technique are presented in Fig. 6, for σ_z, which demonstrate trends that are apparent across roughness parameters (Fig. 4). Supplementing the analysis of roughness spatial variability using CV (Figs. 4 and 5), boxplots enable examination of the evolution of the median value of a roughness parameter with window size increases. For roughness statistics calculated at small window sizes, the variability was larger than that at larger window sizes (Fig. 6), which echoes previous observations using CV (Figs. 4 and 5). Visually both the median values and the variability in

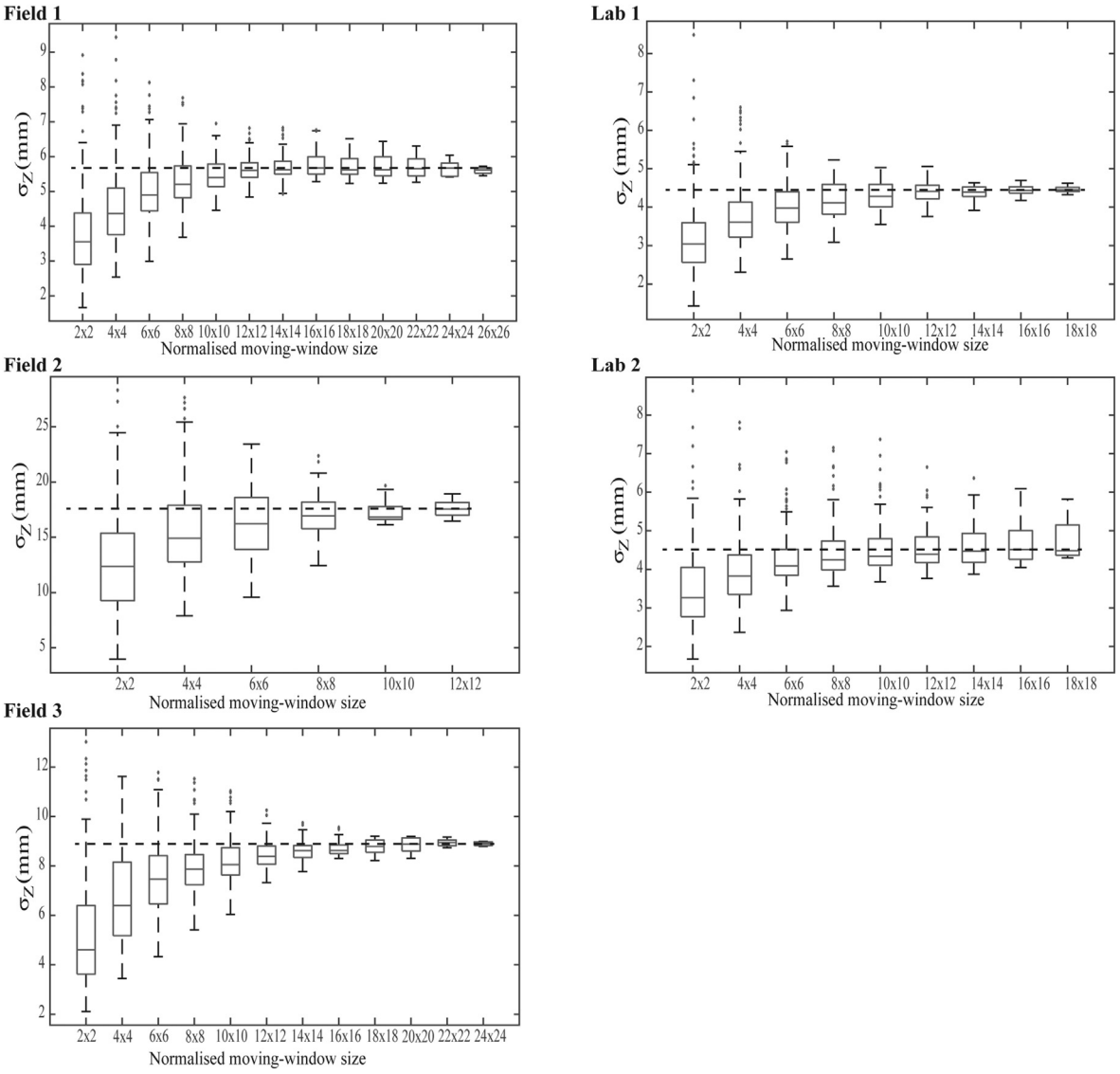

Fig. 6. Standard deviation of bed elevations (σ_z) for all datasets, (Field DEMs left column, Lab DEMs occupy the right column), calculated at different moving-window sizes normalised in both directions by D_{50A}. Horizontal line in the boxplot represents the median value for each DEM size and whiskers display the variability in results. Dashed lines were added to help visualise the plateauing in σ_z with window size increases.

statistics (e.g., boxplot whiskers) plateau between 14 and 18 × D_{50A} for all patches (Fig. 6). These plateaus were confirmed statistically using 95% confidence intervals and a paired *t*-test. The plateaus indicate the window (hence DEM) size is adequately detecting the topographic information under the scale of interest. Figs. 5 and 6 suggest once the DEM size exceeds between 16 and 18 × D_{50A} in both directions in the field DEMs, and smaller sizes between 14 and 16 × D_{50A} in the laboratory, information derived from DEMs is deemed to provide a suitable indication of the overall surface roughness with little effect due to surface variability. Noticeably, Field 2 (Figs. 5b and 6b) began to plateau at smaller window sizes (10–12 × D_{50A}) than the other two field DEMs. However, Field 2 was the patch examined with the coarsest sediment and the smallest normalised patch size (Table 1), which may impede effective plateau identification.

4.3. Effects of Grid spacing on Roughness Parameterisation

Fig. 7 presents results of varying DEM grid spacing on two roughness statistics, σ_z and *I0*, which have been chosen to reflect the patterns observed across parameters (Fig. 4). For this analysis, only grid spacing was varied, whilst parameters were calculated over the complete DEM size (i.e., patch size).

Fig. 7 shows minimal differences between using a 0.35 mm and a 1 mm grid spacing, which was observed across all patches. 1 mm corresponds to the size of the smallest surface grains identified in this study, which also corresponds to a ratio of between 1 and 20 and 1 to 50 when compared with D_{50A} (cf. Table 1). For this reason, small grid sizes are presented in absolute values (i.e., not normalised by D_{50A}). Fig. 7a displays stable σ_z with changes to grid spacing exceeding 1 mm, up to a grid size equal to $D_{50A,}$ for all patches, apart from Field 2, which displays differences at a grid spacing equally the D_{50A} value. However, there are evident differences in inclination index (*I0*) at the coarser spacing, with grid spacing exceeding 1 mm providing fluctuating values, generally negative, and therefore unable to detect surface grain imbrication. This echoes previous observations of *I0* (and skewness) being more variable spatially within a patch than σ_z (Fig. 4), and thus requires smaller grid spacing for roughness characterisation.

5. Discussion

5.1. Surface variability and roughness parameters

Previous studies using gravel-bed DEMs for roughness parameterisation often differ in terms of the DEM size and grid spacing used for analysis. Common to all studies however, is the assumption that parameters derived from DEMs are reliable measurements of the surface. We show that accounting for spatial variability of the surface

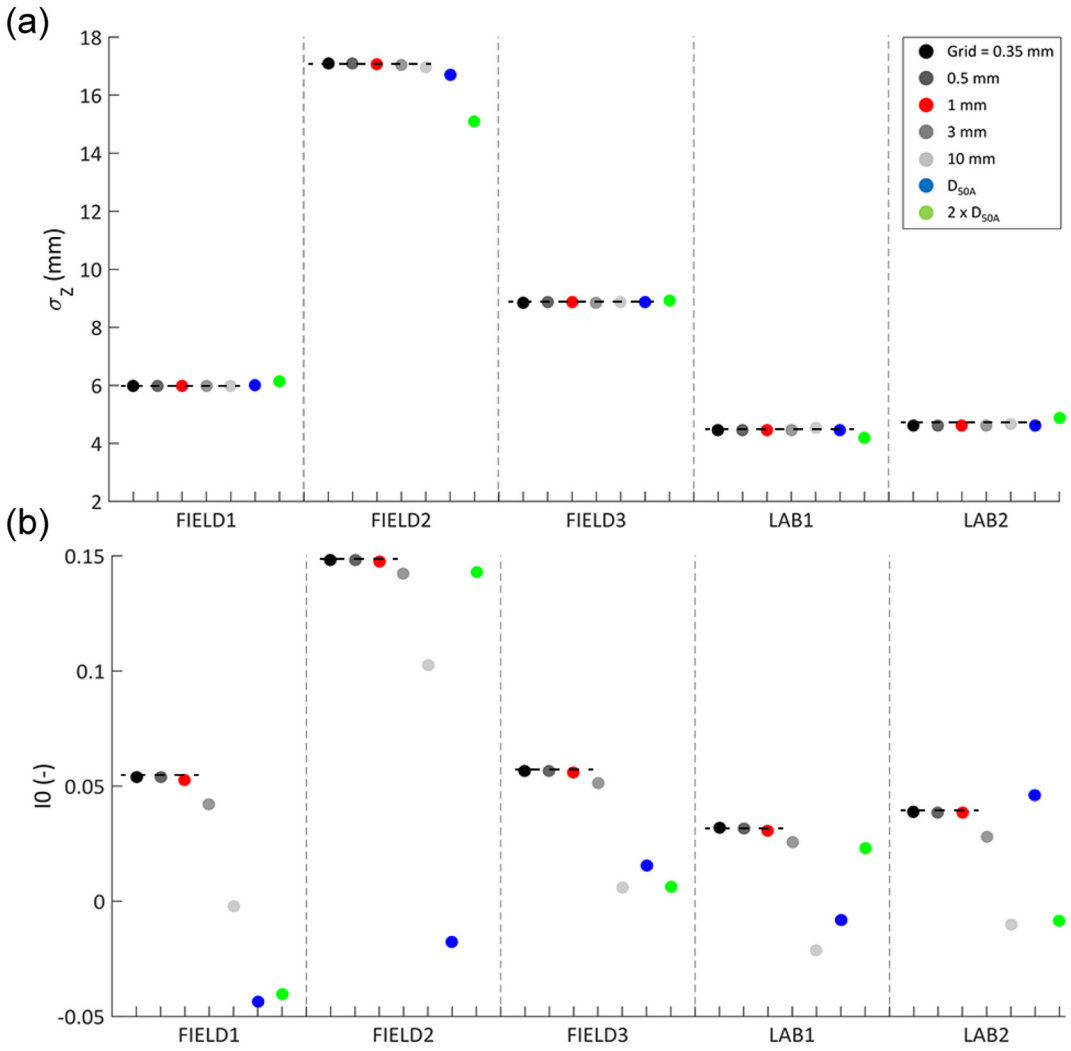

Fig. 7. The effect of grid spacing for all datasets on the (a) standard deviation (σ_z) and (b) inclination index in the flow direction (*I0*). The selection of the two surface metrics was based on the consideration that σ_z and *I0* encompass the patterns observed over all parameters. Horizontal lines were added to help visualise the similarities in data points. D_{50A} values are presented in Table 1.

is important, as it has implicit connections with analytical requirements (e.g., the required DEM size and grid spacing).

In this study, spatial variability in roughness parameters is quantified to provide deeper insights into the fundamentals required for DEM analysis. Novel results obtained show that spatial variability in roughness parameters exists across a gravel patch, in addition to spatial variability in sediment size, as processes shaping alluvial beds naturally result in surface heterogeneity at all scales (e.g., Graham et al., 2010; Nelson et al., 2014; Scown et al., 2015). This complements previous observations of spatial variability in sediment size. Besides, results show that roughness parameters differ greatly on their degree of spatial variability within a patch (e.g., the vertical shift between roughness parameters shown in Fig. 4).

Roughness parameters with the lowest and most consistent variance over window size increases (e.g., horizontal roughness lengths and σ_z) are deemed the parameters adequate to provide robust measures of roughness over a patch. However, certain roughness parameters display high variance (e.g., skewness), with fluctuations in this parameter reflecting spatial variability in particle arrangement (Aberle and Nikora, 2006). Similarly, large fluctuations in inclination index for a given window size indicate heterogeneous grain imbrication (Fig. 4).

5.2. DEM size

Although differing in their degree of spatial variability, all roughness parameters examined show a consistent reduction in spatial variability with window size increases (Fig. 4). Thus, one can use measurements of spatial variability to identify a suitable DEM size that ensures roughness parameters independent of the surface heterogeneity (e.g., Scown et al., 2015, 2016). A similar approach was used by Graham et al. (2010) to determine a suitable measurement size for maximising the accuracy of image-based grain size measurements.

Fig. 5 shows a greater control of window size (hence DEM size) on roughness statistics than the orientation (shape) of the window. Overall, the orientation of measurements does not have a clear influence on the roughness statistics, unless the surface is clearly anisotropic. Therefore, square moving windows should be used for analysis of gravel bed spatial variability, in order to reduce the effect of anisotropy.

Findings of a reduction in CV with increases in window size (Figs. 4 and 5) are in line with a field-based study of roughness length and bed shear stress in a coarse-bed channel, which found reduced CV with an increase in sample size (i.e., an increased number of samples collected over an increased spatial coverage) (Cienciala and Hassan, 2016). Once a certain DEM size is reached, at which grain-roughness information is measured, CV may reduce again due to the presence of bedforms or larger scale roughness elements (Fig. 5). This supports the theory of gravel patches displaying mixed-fractal behaviour with two scales of roughness, whereby bedform roughness is represented by a fractal band exceeding the largest grains (Robson et al., 2002; Aberle and Nikora, 2006; Bergey, 2006; Qin and Ng, 2012; Noss and Lorke, 2016). Although CV reduces following a plateau, gravel patches display variance continually due to the lack of uniformity in the nature of a gravel-bed surface. This lack of uniformity leads to topographic variability both within and between patches analysed in this study, due to differences in sorting, packing, burial, imbrication, shape and size of the sediment (Graham et al., 2010).

The plateau in variance observed in the field DEMs occurred at larger sizes, due to poorly sorted sediment (Table 1) and the increased prevalence of small-scale bedforms in the field (seen in Fig. 2). Bedforms can contribute to an increased surface complexity in comparison to the uniform laboratory DEMs, with variance plateauing at smaller sizes (Bertin and Friedrich, 2016).

As mentioned previously, plateaus were observed when the median values become stable and variability remains consistent as window size increases further (Figs. 5 and 6). These observed plateaus were confirmed statistically, using 95% confidence intervals to assess variability (also used in work by Cienciala and Hassan (2016) to assess spatial variability in data relating to sample size) and a paired *t*-test to assess for statistical differences between mean values for the data at each moving-window size. The statistical confirmation used both methods, as in some parameters the median values plateaued, however variability fluctuated, and observed thresholds considered both of these factors to be stable for estimation of an appropriate DEM size. Therefore, in certain roughness parameters, such as skewness and σ_z in Field 2, a plateau was not observed, possibly due to a small DEM size compared to D_{50A} and high spatial variability across the surface.

5.3. Grid spacing

A previous study by Scown et al. (2015), investigating the effect of DEM size on floodplain topography did not consider the effect of grid spacing on the outputs. In contrast, this work finds grid spacing to have an effect on roughness statistics (Fig. 7).

The lack of differences between 0.35 mm and 1 mm grid spacing for all roughness parameters measured in this study (Fig. 7), suggests these grid spacings are adequately capturing the grain roughness for a range of sediment size (D_{50A} = [19–47 mm]) (Hodge et al., 2009a; Hodge et al., 2009b). Throughout the DEM size analysis a grid spacing of 1 mm was used, as this is already degraded from a point spacing of ~0.2 mm in point clouds (Table 1) and provided the best DEM quality results obtainable, with reasonable efficiency. Furthermore, this is the grid spacing that other researchers have used (Hodge et al., 2009a; Curran and Waters, 2014; Bertin et al., 2017).

Exceeding the 1 mm grid spacing affects the results, suggesting using these resolutions do not provide suitable grain-roughness statistics and even induce errors (Milenković et al., 2015). The differences in values observed at these grid spacings is due to complex surface topography being lost, or the spatial variability of the surface being non-identifiable (Buffin-Bélanger et al., 2006; Hodge et al., 2009a). Previous studies have found that using a coarser grid spacing of 5 mm prevented the identification of the spatial variability of a sediment surface (Buffin-Bélanger et al., 2006). For example, coarser grid spacing may pick up bedform roughness, reflecting the variability between humps and hollows of bedforms, and warping the grain-scale statistics. These differences at larger grid spacing are particularly evident in inclination index (Fig. 7b) with values of 0 or negative, which indicates there is no imbrication of sediment grains. This suggests larger grid spacing does not identify grain imbrications that are observed for resolutions below 3 mm.

6. Implications of the research

6.1. Measurement of roughness spatial variability to explain surface processes

Assessing spatial variability of a gravel-bed surface is of importance to studies investigating the interactions between sediment and flow, for instance to explain measured spatial differences in sediment transport (Haschenburger and Wilcock, 2003; Casas et al., 2010). Using patch-scale DEMs and a moving-window technique, it is shown that using parameters such as σ_z and roughness lengths from structure functions, although providing stable measures of roughness, may be inappropriate for spatial-variability characterisation. In particular, Fig. 4 has highlighted the need to holistically represent roughness using a range of roughness parameters, such as those presented in this study, to gain an understanding of the surface roughness and its spatial variability. Contrasting with σ_z, grain imbrication and bed-elevation skewness vary greatly within a patch (Fig. 4), which has important implications when deciding which bed parameters to measure to explain process heterogeneity, such as sediment transport.

6.2. Suitable DEM size for grain-roughness characterisation

We suggest that a DEM size exceeding $16 \times D_{50A}$ in both directions (which is the modal plateau value from all roughness parameters and DEMs) is required to provide reliable grain-roughness statistics. This recommendation of DEM size is supported by our previous work (Bertin et al., 2017, Figs. 2 and 6), whereby the analysis of roughness spatial variability was extended to 35 DEMs and included DEMs collected in a laboratory flume by Aberle and Nikora (2006) and the Waimakariri River (Smart et al., 2004).

At first look, the plateaus obtained appear lower than the value of $21 \times D_{50}$ deemed appropriate for patch size in previous literature (Ockelford and Haynes, 2013). A possible reason is that sediment size in our study is based on the armour (i.e., surface) layer, whilst we believe Ockelford and Haynes (2013) refer to the subsurface (or bulk mixture) D_{50} (based on D_{50} of 4.8 mm). To allow comparison, the thresholds obtained here need to be converted from only considering the armour layer, to the subsurface layer too. Assuming an armouring ratio of 2 (i.e. $D_{50A}/D_{50} = 2$), which has been measured for our experimental beds (cf. Table 1) and observed in gravel-bed rivers in the field (Oldmeadow and Church, 2006), the thresholds in this paper would be between 28 and $36 \times D_{50}$. Therefore these thresholds are actually higher than the $21 \times D_{50}$ suggested by Ockelford and Haynes (2013) and our results stress the importance of sediment sorting and bedform prevalence (i.e., spatial organisation) on these thresholds. Further, this highlights the importance of a required uniformity within research for data analysis procedures in order to facilitate comparisons between studies. This statement supports a view in larger-scale studies, which, in order to delineate different features and scales of roughness across a floodplain, have stated that research requires an automated process to extract quantitative data from data of varying quality (Bertoldi et al., 2012). Recommendations such as those presented here are a step towards achieving this.

Similar to this patch-scale work, Scown et al. (2016) found spatial organisation of a surface and DEM size to influence measurements of floodplain topography and analytical requirements. The fact that the same findings have been observed at two vastly different spatial scales of fluvial surfaces (i.e., from mm to km) is further evidence of a continuum of roughness scales in the environment. Both studies also support the idea that analysis of roughness spatial variability is effective in detecting transitions between scales, which is an avenue of research that could benefit from further exploration.

6.3. Suitable grid spacing for grain-roughness characterisation

The finding that grid spacing exceeding 1 mm is not able to identify grain imbrication has implications for the collection of high-resolution topographic data. For the goal of grain-roughness parameterisation, it is important to obtain a resolution that can adequately detect individual grains, yet with the ability to be efficiently computated (e.g., use of a 1 mm grid spacing rather than 0.2 mm in this study). Therefore the researcher should make a decision in regards to computation time, and a compromise made between using a sufficient grid size (e.g., 1 mm) and data quality desired. A major benefit of high resolution data is that the data can be resampled at differing spacing required by the analysis (Ockelford and Haynes, 2013). Future work could explore the effect of grid spacing on larger patches than those presented here (as well as at floodplain scale, which was not formerly conducted), and determine requirements for analysing bedform roughness.

7. Conclusions

In this study, an analytical process based on roughness spatial variability was used, aimed to improve the understanding of how to analyse topographic data for gravel-bed roughness parameterisation, which is of increasing relevance for fluvial research. We have found that the scale of roughness under investigation is a vital pre-analysis decision required by the researcher, as the surface morphology and structure can influence the analysis required for a DEM. The study focused on grain-roughness characterisation using gravel-patch DEMs.

Firstly, spatial variability in microtopography across a gravel-bed was adequately quantified using the moving-window analysis technique. This evident variability suggests that one single roughness parameter, such as standard deviation, is not sufficient to represent grain-scale roughness; therefore using a combination of roughness parameters, as presented in this study, provides a more holistic view of surface complexity.

Secondly, the size of DEM influences the calculated roughness statistics, with a plateau in variance observed between 16 and $18 \times D_{50A}$ in the field DEMs, and between 14 and $16 \times D_{50A}$ in the laboratory, suggesting these DEM sizes provide robust measures of surface roughness. Differences in the effect of DEM size between laboratory and field were found to be due to multiple scales of roughness present on a gravel surface and differing sediment sorting.

Minimal differences between grid spacing below 1 mm indicate that the same quality results can be obtained at less computation time, using the coarser grid spacing. However, it is essential for researchers to consider the scale of investigation, as using coarser resolutions will cause a loss of topographic information and inadequately represent grain roughness, rather focusing on roughness of larger scales, such as bedform roughness. This was particularly apparent when quantifying grain imbrication, which failed for grid spacings exceeding 1 mm.

Based on this study, which considered patches of varying sediment size, surface morphology and from different environments, we suggest for grain-scale roughness research using a DEM size and therefore patch size exceeding $16 \times D_{50A}$ in both directions and using a grid spacing of 1 mm or below. As these insights come from a range of environments and sediment, future research using guidance presented in this paper, will provide adequate roughness parameterisation and also this will facilitate comparisons between studies.

Acknowledgements

The study was partly funded by the Marsden Fund (Grant no. UOA1412), administered by the Royal Society of New Zealand. The authors would like to thank anonymous reviewers whose constructive comments helped to improve the manuscript.

References

Aberle, J., Nikora, V., 2006. Statistical properties of armored gravel bed surfaces. Water Resour. Res. 4211, W11414. https://doi.org/10.1029/WR004674.
Aberle, J., Smart, G., 2003. The influence of roughness structure on flow resistance on steep slopes. J. Hydraul. Res. 413, 259–269.
Baewert, H., Bimböse, M., Bryk, A., Rascher, E., Schmidt, K., Morche, D., 2014. Roughness determination of coarse grained alpine river bed surfaces using Terrestrial Laser Scanning data. Zeitschrift Für Geomorphologie 581 (Supplementary Issues), 81–95.
Barber, M.E., Grings, F.M., Álvarez-Mozos, J., Piscitelli, M., Perna, P.A., Karszenbaum, H., 2016. Effects of spatial sampling interval on roughness parameters and microwave backscatter over agricultural soil surfaces. Remote Sens. 86, 458.
Bergey, E.A., 2006. Measuring the surface roughness of stream stones. Hydrobiologia 5631, 247–252.
Bertin, S., Friedrich, H., 2014. Measurement of gravel-bed topography: Evaluation study applying statistical roughness analysis. J. Hydraul. Eng. 1403, 269–279.
Bertin, S., Friedrich, H., 2016. Field application of close-range digital photogrammetry (CRDP) for grain-scale fluvial morphology studies. Earth Surf. Process. Landf. https://doi.org/10.1002/esp.3906.
Bertin, S., Friedrich, H., Delmas, P., Chan, E., Gimel'farb, G., 2015. Digital stereo photogrammetry for grain-scale monitoring of fluvial surfaces: Error evaluation and workflow optimisation. ISPRS J. Photogramm. Remote Sens. 101, 193–208.
Bertin, S., Groom, J., Friedrich, H., 2017. Isolating roughness scales of gravel-bed patches. Water Resour. Res. 53, 6841–6856. https://doi.org/10.1002/2016WR020205.
Bertoldi, W., Piegay, H., Buffin-Bélanger, T., Graham, D., Rice, S., 2012. Applications of close-range imagery in river research. In Fluvial Remote Sensing for Science and Management, pp. 341–366 https://doi.org/10.1002/9781119940791.ch15.
Bouguet, J.-Y., 2010. Camera Calibration Toolbox for Matlab, Caltech, Pasadena, California. Avaliable at:. http://vision.caltech.edu/bouguetj/calib_doc/.
Buffin-Bélanger, T., Rice, S., Reid, I., Lancaster, J., 2006. Spatial heterogeneity of near-bed hydraulics above a patch of river gravel. Water Resour. Res. 424.

Casas, M., Lane, S., Hardy, R., Benito, G., Whiting, P., 2010. Reconstruction of Subgrid-scale topographic variability and its effect upon the spatial structure of three-dimensional river flow. Water Resour. Res. 463.
Cienciala, P., Hassan, M.A., 2016. Sampling variability in estimates of flow characteristics in coarse-bed channels: Effects of sample size. Water Resour. Res. 52, 1899–1922. https://doi.org/10.1002/2015WR017259.
Coleman, S.E., Nikora, V.I., Aberle, J., 2011. Interpretation of alluvial beds through bed-elevation distribution moments. Water Resour. Res. 4711, W11505. https://doi.org/10.1029/2011WR010672.
Crowder, D.W., Diplas, P., 1997. Sampling heterogeneous deposits in gravel-bed streams. J. Hydraul. Eng. 12312, 1106–1117.
Curran, J.C., Waters, K.A., 2014. The importance of bed sediment sand content for the structure of a static armor layer in a gravel bed river. J. Geophys. Res. Earth Surf. 1197, 1484–1497.
Detert, M., Weitbrecht, V., 2012. Automatic object detection to analyze the geometry of gravel grains–a free stand-alone tool. Proceedings of River Flow. 2012, pp. 595–600.
Erskine, R.H., Green, T.R., Ramirez, J.A., MacDonald, L.H., 2007. Digital elevation accuracy and grid cell size: effects on estimated terrain attributes. Soil Sci. Soc. Am. J. 714, 1371–1380.
Fehr, R., 1987. Geschiebeanalysen in Gebirgsflüssen: Umrechnung Und Vergleich Von Verschiedenen Analyseverfahren, Versuchsanst. für Wasserbau, Hydrologie u. Glaziologie.
Florinsky, I.V., Kuryakova, G.A., 2000. Determination of Grid size for digital terrain modelling in landscape investigations—exemplified by soil moisture distribution at a micro-scale. Int. J. Geogr. Inf. Sci. 148, 815–832.
Gao, J., 1998. Impact of sampling intervals on the reliability of topographic variables mapped from grid DEMs at a micro-scale. Int. J. Geogr. Inf. Sci. 128, 875–890.
Gimel'farb, G., 2002. Probabilistic regularisation and symmetry in binocular dynamic programming stereo. Pattern Recog. Lett. 234, 431–442.
Graham, D.J., Rollet, A., Piégay, H., Rice, S.P., 2010. Maximizing the accuracy of image-based surface sediment sampling techniques. Water Resour. Res. 462, W02508. https://doi.org/10.1029/2008WR006840.
Grieve, S.W., Mudd, S.M., Milodowski, D.T., Clubb, F.J., Furbish, D.J., 2016. How does grid-resolution modulate the topographic expression of geomorphic processes? Earth Surf. Dyn. 4, 627–653.
Haschenburger, J.K., Wilcock, P.R., 2003. Partial transport in a natural gravel bed channel. Water Resour. Res., 391 https://doi.org/10.1029/2002WR001532.
Heritage, G.L., Milan, D.J., Large, A.R., Fuller, I.C., 2009. Influence of survey strategy and interpolation model on DEM quality. Geomorphology 1123, 334–344.
Hodge, R., Brasington, J., Richards, K., 2009a. Analysing laser-scanned digital terrain models of gravel bed surfaces: linking morphology to sediment transport processes and hydraulics. Sedimentology 567, 2024–2043.
Hodge, R., Brasington, J., Richards, K., 2009b. In situ characterization of grain-scale fluvial morphology using Terrestrial Laser Scanning. Earth Surf. Process. Landf. 347, 954–968.
Jia, Z., Hu, Z., 2015. Evaluation methods of material surface macro-roughness. Mater. Res. Innov. 19 (S8-293-S8-296).
Lane, S.N., 2005. Roughness–time for a re-evaluation? Earth Surf. Process. Landf. 302, 251–253.
Lane, S., James, T., Crowell, M., 2000. Application of digital photogrammetry to complex topography for geomorphological research. Photogramm. Rec. 1695, 793–821.
Laronne, J., Carson, M., 1976. Interrelationships between bed morphology and bed-material transport for a small, gravel-bed channel. Sedimentology 231, 67–85.
Mao, L., Cooper, J.R., Frostick, L.E., 2011. Grain size and topographical differences between static and mobile armour layers. Earth Surf. Process. Landf. 3610, 1321–1334.
Martinez-Agirre, A., Álvarez-Mozos, J., Giménez, R., 2016. Evaluation of surface roughness parameters in agricultural soils with different tillage conditions using a laser profile meter. Soil Tillage Res. 161, 19–30.
Milan, D.J., Heritage, G.L., Large, A.R., Fuller, I.C., 2011. Filtering spatial error from dems: implications for morphological change estimation. Geomorphology 1251, 160–171.
Milenković, M., Pfeifer, N., Glira, P., 2015. Applying Terrestrial Laser Scanning for soil surface roughness assessment. Remote Sens. 72, 2007–2045.
Millane, R., Weir, M., Smart, G., 2006. Automated analysis of imbrication and flow direction in alluvial sediments using laser-scan data. J. Sediment. Res. 768, 1049–1055.
Morvan, H., Knight, D., Wright, N., Tang, X., Crossley, A., 2008. The concept of roughness in fluvial hydraulics and its formulation in 1D, 2D and 3D numerical simulation models. J. Hydraul. Res. 462, 191–208.
Nelson, P., Bellugi, D., Dietrich, W., 2014. Delineation of river bed-surface patches by clustering high-resolution spatial grain size data. Geomorphology 205, 102–119. https://doi.org/10.1016/j.geomorph.2012.06.008.
Nikora, V.I., Goring, D.G., Biggs, B.J., 1998. On gravel-bed roughness characterization. Water Resour. Res. 343, 517–527.
Noss, C., Lorke, A., 2016. Roughness, resistance, and dispersion: relationships in small streams. Water Resour. Res. 524, 2802–2821.
Ockelford, A., Haynes, H., 2013. The impact of stress history on bed structure. Earth Surf. Process. Landf. 387, 717–727.
Oldmeadow, D.F., Church, M., 2006. A field experiment on streambed stabilization by gravel structures. Geomorphology 783, 335–350.
Pearson, E., Smith, M., Klaar, M., Brown, L., 2017. Can high resolution 3D topographic surveys provide reliable grain size estimates in gravel bed rivers? Geomorphology 293, 143–155.
Piedra, M.M., Haynes, H., Hoey, T.B., 2012. The spatial distribution of coarse surface grains and the stability of gravel river beds. Sedimentology 593, 1014–1029.
Powell, D.M., Ockelford, A., Rice, S.P., Hillier, J.K., Nguyen, T., Reid, I., Tate, N., Ackerley, D., 2016. Structural properties of mobile armors formed at different flow strengths in gravel-bed rivers. J. Geophys. Res. Earth Surf. 1218, 1494–1515.
Qin, J., Ng, S., 2012. Estimation of effective roughness for water-worked gravel surfaces. J. Hydraul. Eng. 13811, 923–934.
Rice, S.P., Buffin-Bélanger, T., Reid, I., 2014. Sensitivity of interfacial hydraulics to the microtopographic roughness of water-lain gravels. Earth Surf. Process. Landf. 392, 184–199.
Robson, B., Chester, E., Barmuta, L., 2002. Using fractal geometry to make rapid field measurements of riverbed topography at ecologically useful spatial scales. Mar. Freshw. Res. 536, 999–1003.
Scown, M.W., Thoms, M.C., De Jager, N.R., 2015. Measuring floodplain spatial patterns using continuous surface metrics at multiple scales. Geomorphology 245, 87–101.
Scown, M.W., Thoms, M.C., De Jager, N.R., 2016. An index of floodplain surface complexity. Hydrol. Earth Syst. Sci. 201, 431–441.
Smart, G.M., Duncan, M.J., Walsh, J.M., 2002. Relatively rough flow resistance equations. J. Hydraul. Eng. 1286, 568–578.
Smart, G., Aberle, J., Duncan, M., Walsh, J., 2004. Measurement and analysis of alluvial bed roughness. J. Hydraul. Res. 423, 227–237.
Smith, M.W., 2014. Roughness in the Earth Sciences. Earth-Sci. Rev. 136, 202–225.
Smith, M., Vericat, D., Gibbins, C., 2012. Through-water terrestrial laser scanning of gravel beds at the patch scale. Earth Surf. Process. Landf. 374, 411–421.
Stähly, S., Friedrich, H., Detert, M., 2017. Size ratio of fluvial grains' intermediate axes assessed by image processing and square-hole sieving. J. Hydraul. Eng. 143 (6), 06017005.
Trevisani, S., Cavalli, M., 2016. Topography-based flow-directional roughness: potential and challenges. Earth Surf. Dyn. 4, 343–358.
Tuijnder, A.P., Ribberink, J.S., 2012. Experimental observation and modelling of roughness variation due to supply-limited sediment transport in uni-directional flow. J. Hydraul. Res. 505, 506–520.
Wilcock, P., 1996. Estimating local bed shear stress from velocity observations. Water Resour. Res. 3211, 3361–3366.
Zhang, Z., 2000. A flexible new technique for camera calibration. IEEE Trans. Pattern Anal. Mach. Intell. 2211, 1330–1334.
Zhang, W., Montgomery, D.R., 1994. Digital elevation model grid size, landscape representation, and hydrologic simulations. Water Resour. Res. 304, 1019–1028.